

Supporting Information

Electrotunable Nanoplasmonics for Amplified Surface Enhanced Raman Spectroscopy

Ye Ma^{1,2}, Debabrata Sikdar^{1,3}, Aleksandra Fedosyuk¹, Leonora Velleman¹, Daniel J. Klemme⁴, Sang-Hyun Oh⁴, Anthony R.J. Kucernak¹, Alexei A. Kornyshev^{1,5*}, Joshua B. Edel^{1*}

¹Department of Chemistry, Imperial College London, Molecular Sciences Research Hub, White City Campus, London W12 0BZ, UK

²School of Materials Science and Engineering, Ocean University of China, Qingdao, 266100, China

³Department of Electronics and Electrical Engineering, Indian Institute of Technology Guwahati, Guwahati-781039, India

⁴Department of Electrical and Computer Engineering, University of Minnesota, Minneapolis, Minnesota 55455, USA

⁵Thomas Young Centre for Theory and Simulation of Materials, Imperial College London, South Kensington Campus, London SW7 2AZ, UK

Correspondence: a.kornyshev@imperial.ac.uk, joshua.edel@imperial.ac.uk

Table of Contents

1. Electrochemical cell
2. Gold nanoparticles
3. The influence of electrolyte on nanoparticle stability in bulk solution
4. Determine the potential of zero charge
5. Cyclic voltammogram
6. Surface enhanced Raman spectroscopic intensity mapping and spectra overlay
7. The influence of pH on nanoparticle stability and nanoparticle array density
8. Dip depth of reflectance spectra under different potentials
9. Time-dependant dip depth during the assembling
10. Reversibility
11. Calculation of the enhancement factor
12. Detecting multiple analytes through surface enhanced Raman spectroscopy
13. Raman spectra of MBA functionalized nanoparticle array at the solid liquid interface in serum

1. Electrochemical cell

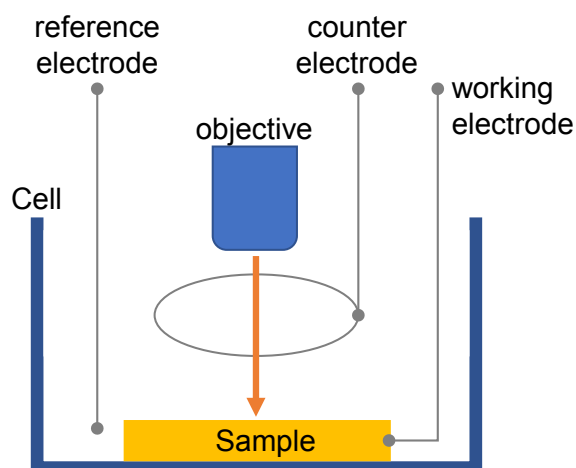


Figure S 1 A planar 125 nm thick Ag substrate with a 5 nm TiN coating acts as the working electrode of an electrochemical cell. A ring-shaped Pt counter electrode and an Ag/AgCl wire reference electrode completes the three-electrode electrochemical cell.

2. Au nanoparticles

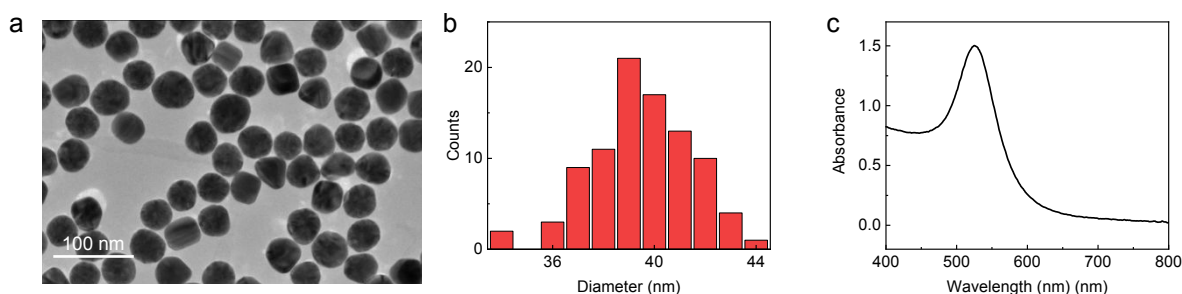


Figure S 2 (a) Transmission electro-microscope (TEM) image of 40 ± 3 nm Au nanoparticles (NPs). (b) Statistics of NP diameter measured from TEM images. (c) UV-vis spectra of NP solution.

3. The influence of electrolyte on NP stability in bulk solution

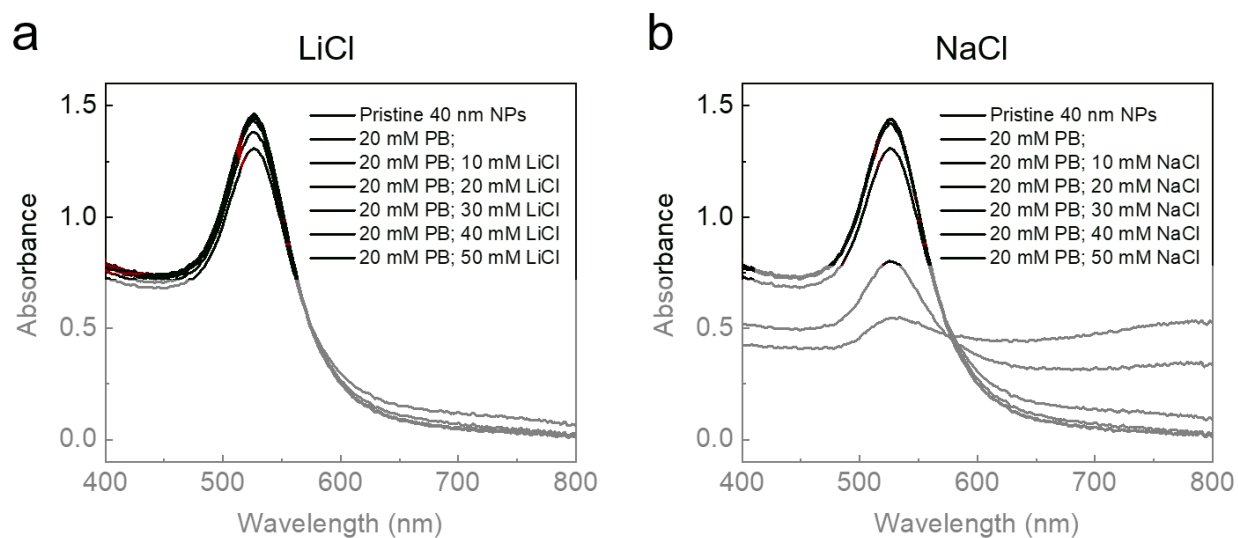


Figure S 3 LiCl (a) and NaCl (b) tolerance of 40 nm MBA functionalized gold NPs with no electrolyte, 20 mM phosphate buffer (PB) and 20 mM PB plus 10 to 50 mM designated LiCl or NaCl. NPs can tolerate higher concentration of LiCl than that of NaCl regarding the prevention of NP aggregation.

4. Determining the potential of zero charge

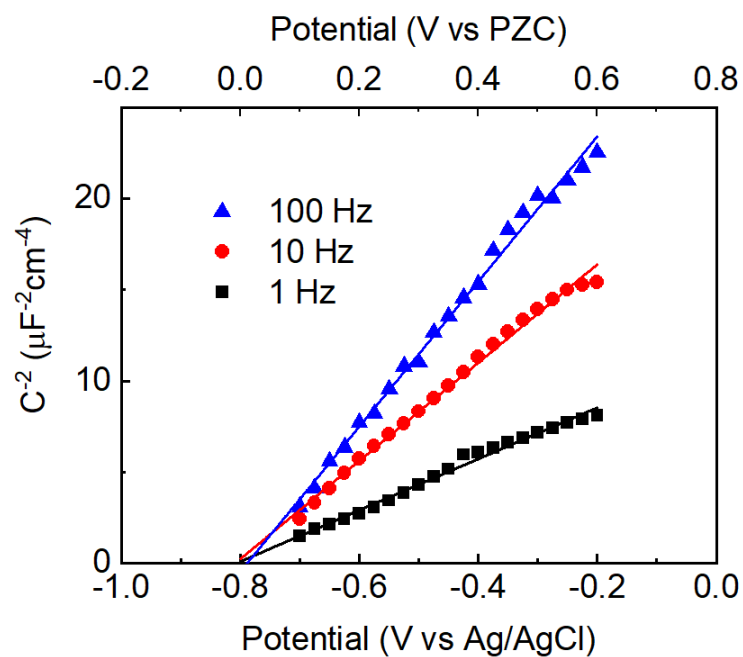


Figure S 4 Mott-Schottky plot for the capacitance of TiN/Ag electrode in 20 mM PBS, 20 mM LiCl aqueous solution, determining PZC as -0.8 V vs Ag/AgCl, under 1, 10, and 100 Hz impedance measurements. All the linear fittings ($C^{-2} \propto E - E_{\text{PZC}} - k_{\text{B}}T/e$) give a similar intercept.

5. Cyclic voltammogram

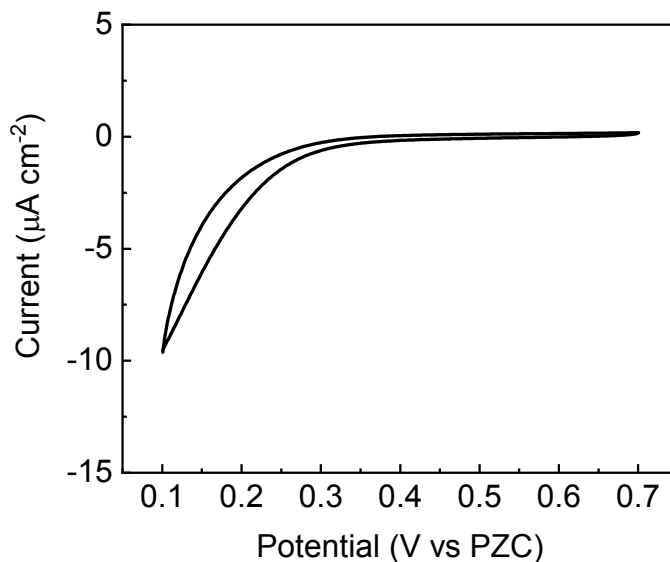


Figure S 5 Cyclic voltammogram of TiN/Ag in 20 mM PBS, 20 mM LiCl aqueous solution with 10 mV/s scanning rate.

6. SERS intensity mapping and spectra overlay

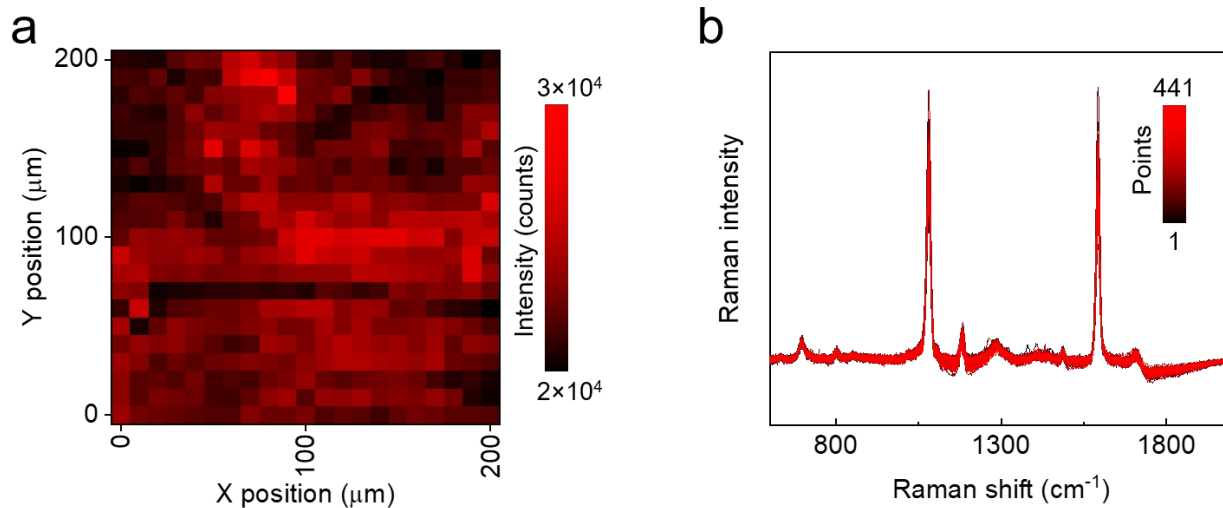


Figure S 6 (a) Intensity mapping of the Raman peak at 1589 cm^{-1} within a $200 \times 200 \mu\text{m}^2$ area on the assembled NP array on TiN/Ag substrate; step size 10 μm . (b) The overlay of the Raman spectra of 21×21 points shown in panel a.

7. The influence of pH on NP stability and NP array density

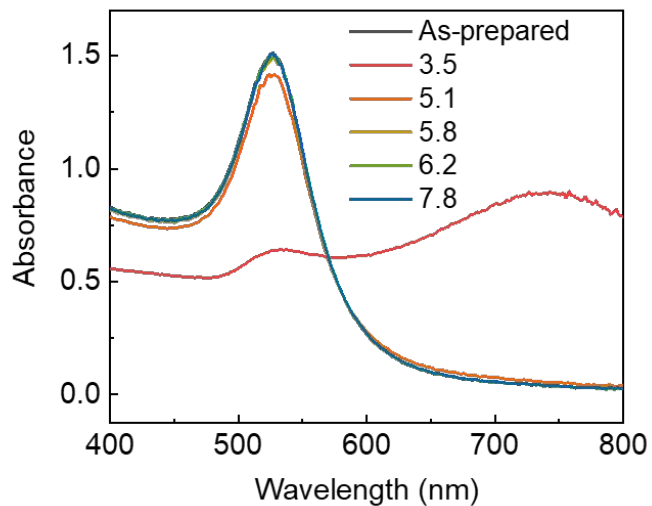


Figure S 7 Stability of colloidal NPs in the bulk solution with respect to pH.

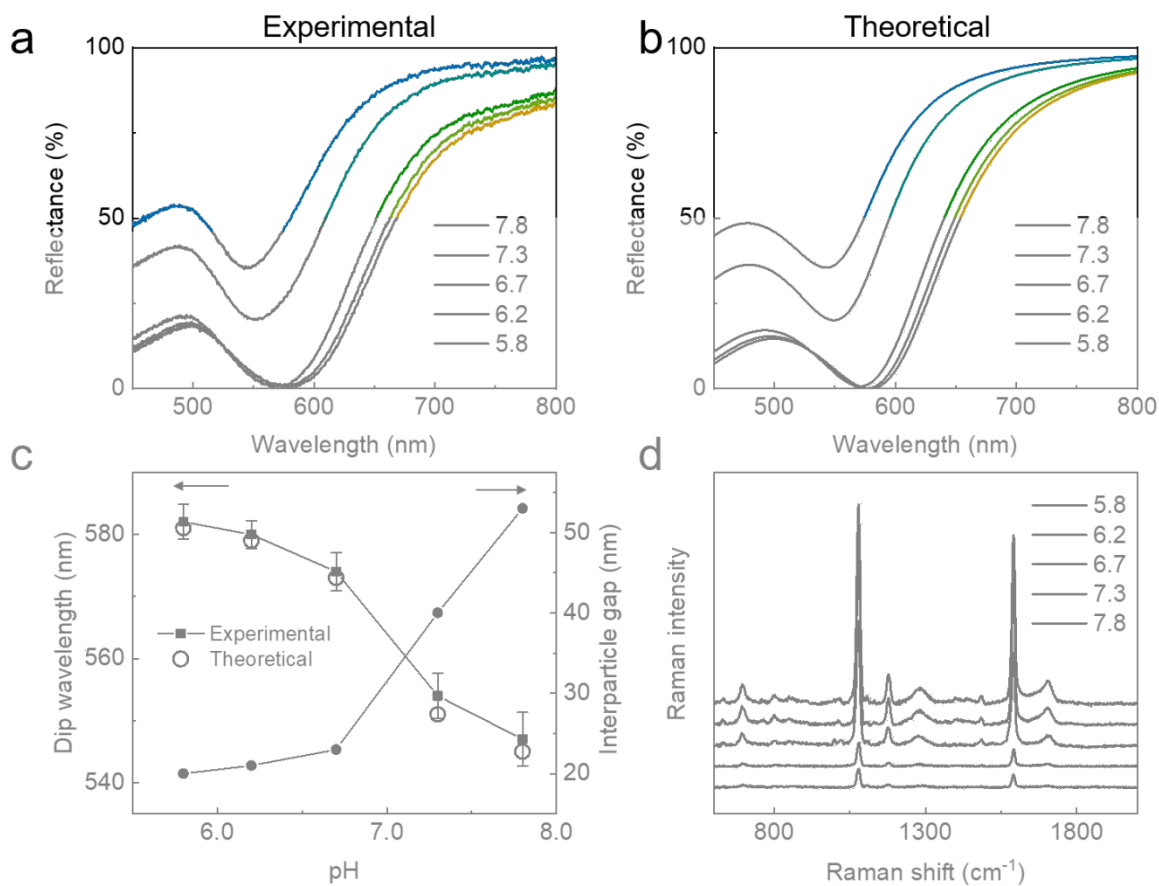


Figure S 8 Influence of pH on the NP assembly at SLI assembled under 0.7 V vs PZC. The experimental (a) and theoretically fitted (b) reflectance curves. (c) Experimental (solid black

squares) and theoretical fitted (empty black circles) dip wavelength extracted from panels (a) or (b), and the theoretically calculated interparticle gaps (solid red circles). (d) Raman spectra of NP array assembled at SLI under different pH environments.

8. Dip depth of reflectance spectra under different potentials

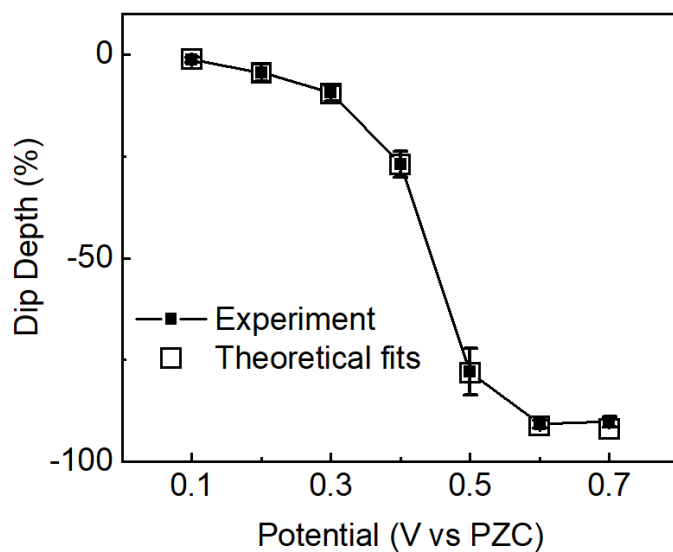


Figure S 9 The experimental (solid) and theoretically fitted (empty) dip depth under 0.1 – 0.7 V vs PZC.

9. Time-dependant dip depth during the assembling

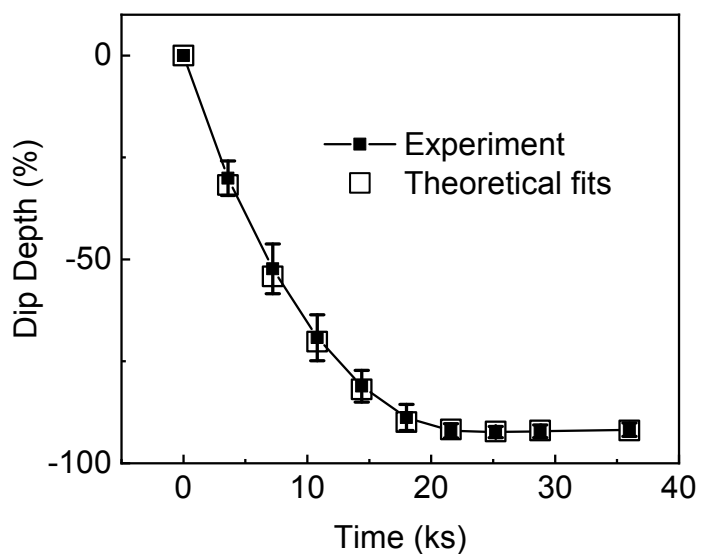


Figure S 10 The time-dependent experimental (solid) and theoretically fitted (empty) dip depth during the assembling of NPs

10. Reversibility

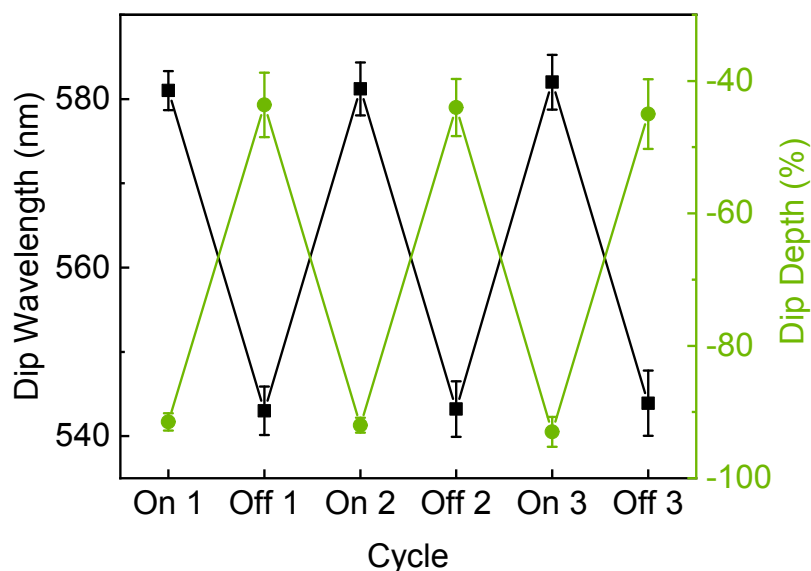


Figure S 11 The dip wavelength and dip depth extracted from experimental reflectance spectra over multiple on/off cycles.

11. Calculation of EF

The experimental EF was calculated according to the equation:

$$EF = \frac{I_{\text{SERS}}/N_{\text{SERS}}}{I_{\text{RS}}/N_{\text{RS}}}$$

where I_{SERS} and I_{RS} denote the intensity of SERS and Raman signals which were directly measured from experiments; N_{SERS} and N_{RS} are the numbers of molecules generating SERS and Raman signals, respectively, which need further calculation.

The general idea of calculating either N_{SERS} or N_{RS} follows: $N = S \times \sigma$, where S is the surface area (cm^2), σ the MBA surface density ($/\text{cm}^2$). Since the S is the same with either SERS or Raman and will be cancelled in EF equation, we will use 1 cm^2 for the ease of calculation.

$N_{\text{RS}} = m \times N_A / M_{\text{MBA}}$, m is the mass of MBA solid on 1 cm^2 , N_A the Avogadro constant, M_{MBA} the molecular weight of MBA.

$$N_{\text{SERS}} = N_{\text{NP}} \times S_{\text{NP}} \times \sigma_{\text{MBA-NP}}$$

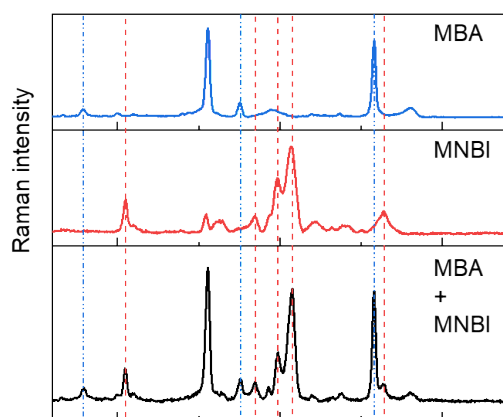
N_{NP} is the number of NPs on 1 cm²: $N_{\text{NP}} = S/S_{\text{NP-lattice}} = S/(\sin 60^\circ \times a^2)$, $S_{\text{NP-lattice}}$ is the hexagonal NP array lattice area, a is the interparticle distance calculated from EMT theory.

S_{NP} is the surface area of single NP: $S_{\text{NP}} = 4\pi r^2$

$\sigma_{\text{MBA-NP}}$ is the MBA density on NP surface, which is taken from previous research.¹

12. Detecting multiple analytes through SERS

a



b

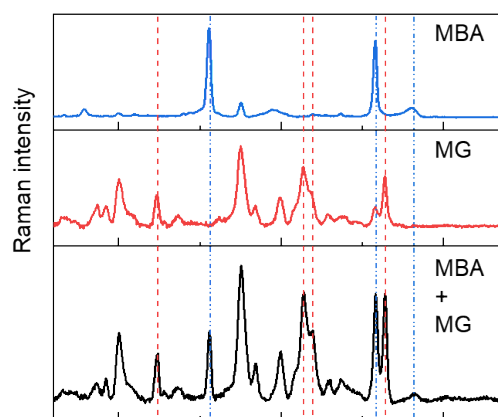


Figure S 12 The detection of different analyte from Raman spectroscopy employing the electro-tunable plasmonic system assembled at 0.7 V vs PZC. (a) The Raman spectra of NP assemblies loading MBA only (blue, top), MNBI only (red, middle) and the mixture of MBA and MNBI (black, bottom). The blue vertical dot-dashed lines indicate the characteristic peaks of MBA, while the red vertical dash lines indicate the characteristic peaks of MNBI. (b) The Raman spectra of NP assemblies loading MBA only (blue, top), MG only (red, middle) and the mixture of MBA and MG (black, bottom). The blue vertical dot-dashed lines indicate the characteristic peaks of MBA, while the red vertical dash lines indicate the characteristic peaks of MG. The above spectra were obtained for 100 nM concentrations of MNBI and MG.

13. Raman spectra of MBA functionalized NP array at SLI in serum solution

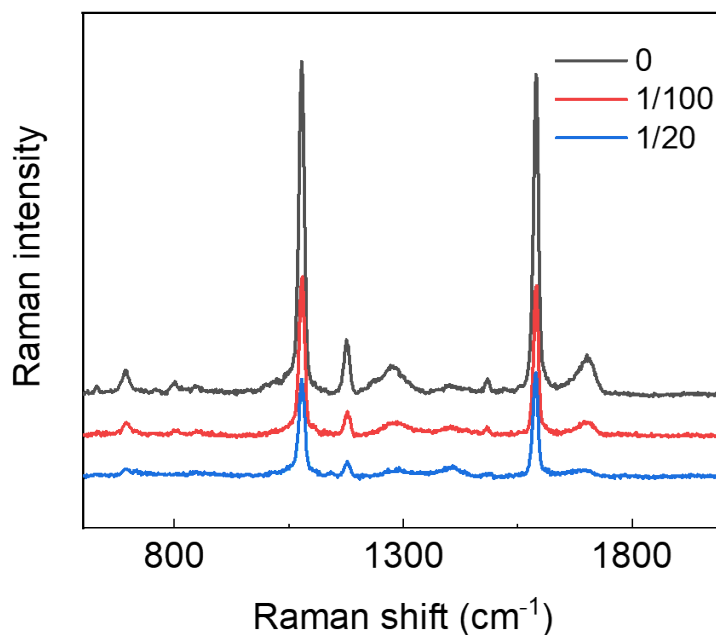


Figure S 13 The Raman spectra of assembled MBA NP array in non-serum and serum solutions. Curves: Black – in 20 mM PB, 20 mM LiCl water solution; Red – in 100 times diluted serum solution; Blue – in 20 times diluted serum solution. For better visibility, the spectra are separated from each other by vertical offsets

Reference:

(1) Velleman, L.; Scarabelli, L.; Sikdar, D.; Kornyshev, A. A.; Liz-Marzan, L. M.; Edel, J. B. Monitoring Plasmon Coupling and SERS Enhancement through *In Situ* Nanoparticle Spacing Modulation. *Faraday Discuss.* **2017**, *205*, 67-83.